Environmental Science & Technology

pubs.acs.org/est

Article

Mortality Risk Associated with Short-Term Exposure to Particulate Matter in China: Estimating Error and Implication

Hao Wang,[#] Peng Yin,[#] Wenhong Fan, Ying Wang, Zhaomin Dong,* Qihong Deng, and Maigeng Zhou

Cite This: *Environ. Sci. Technol.* 2021, 55, 1110−1121

Read Online

ACCESS | Metrics & More | Article Recommendations | Supporting Information

ABSTRACT: Most previous studies used a specific size of particulate matter (PM_x) for dosimetry estimation when determining particulate matter (PM)-associated risk, which precluded the impact of other sizes of PM. Here, we used a multiple-path particle dosimetry model to determine the deposition of PM in human airways and further estimated the associated mortality risk in 205 cities in China. Results showed that the fractions of PM_1, $PM_{1-2.5}$, and coarse PM ($PM_{2.5-10}$) deposited in the tracheobronchial (TB) and pulmonary airways were estimated in ranges of 11.06−12.83, 19.9−26.37, and 5.35−9.81%, respectively. Each 10 $\mu g/m^3$ increase in deposited PM was significantly associated with a nationwide increment of 1.12% (95% confidence interval, CI, 0.77−1.49%) for total nonaccidental mortality. Short-term exposure to PM during 2014−2017 resulted in a nationwide mortality of 98 826 cases/year, with contributions from PM_1, $PM_{1-2.5}$, coarse PM of 37.7, 43.1, and 19.2%, respectively. Our study demonstrated that the estimated mortality counts may be associated with the coefficient of variation of dosimetry estimations. In addition, we revealed the caution should be exercised when interpreting PM_x-associated risk and further reinforced the importance of size distribution in relevant research.

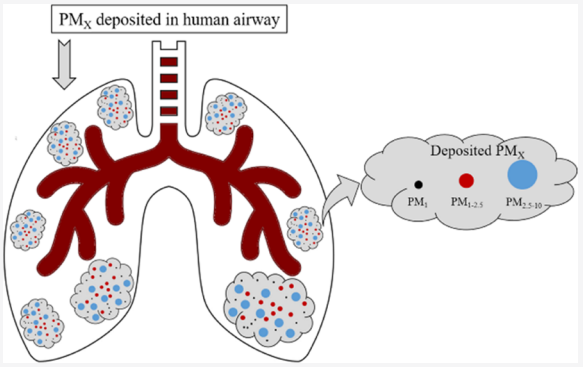

INTRODUCTION

Although a large number of studies have linked particulate matter (PM) exposure and mortality risk,[1−3] most have used a specific size of particulate matter (PM_x) for dosimetry estimation. A characteristic feature of these studies is that they typically preclude the effects of other sizes of PM, while available studies have evidenced that exposure to various sizes of PM (such as PM with aerodynamic diameter < 1 μm (PM_1), PM with aerodynamic diameter < 2.5 μm ($PM_{2.5}$), coarse PM, PM with aerodynamic diameter between 2.5 and 10 μm ($PM_{2.5-10}$), PM with aerodynamic diameter < 10 μm (PM_{10})) can all significantly elevate the cause-specific mortality.[2,4−6] In addition, since PMs of diverse sizes are produced by different mechanisms from various precursors,[7−9] the toxicity of PM may vary.[10] Available studies, although in small number, have indicated that the choices of dosimetry estimation (or dose metric) can significantly influence the associations between PM exposure and adverse effects.[11,12] Hence, size-resolved respiratory doses, rather than PM_x mass concentrations, may be more appropriate to correlate the PM exposure and health effects.[13] The PM deposited in human airways, including the respiratory or circulatory system, depends on size distributions and population characteristics. For example, smaller-size particles are prone to penetrate the lung alveoli and blood vessels, demonstrating the pivotal role of size in PM deposition.[14−17] Additionally, PM deposition exhibits notable discrepancies between population groups, such as males vs females, adults vs children.[18,19] Integrating the deposition patterns in epidemiologic studies can enhance our understanding of PM-related effects.

While about 33% reduction in $PM_{2.5}$ concentration was noted over the last 5 years,[7] PM is still a highly contributing risk factor in China. Earlier studies explored the nationwide mortality risk caused by various sizes of PM exposure.[4,5,20] However, the estimation error in the mortality risk resulted from the choices of dosimetry estimation remains unclear. To address this issue, this study first simulated how PM deposited in the head, tracheobronchial (TB), and pulmonary regions of human airways. Then, a nationwide cause-specific mortality risk attributable to deposited PM was calculated. Finally, we estimated the nationwide mortality risk from PM exposure and evaluated how the choices of dosimetry estimation bias the mortality risk.

Received: July 30, 2020
Revised: December 11, 2020
Accepted: December 14, 2020
Published: December 29, 2020

https://dx.doi.org/10.1021/acs.est.0c05095
Environ. Sci. Technol. 2021, 55, 1110−1121

Table 1. Deposition Fractions of Size-Fractioned Particulate Matter in Different Organs of the Human Body for Different Population Groups[a]

					PM_1 (%)				$PM_{1-2.5}$ (%)				$PM_{2.5-10}$ (%)			
population groups	FRC (mL)	URT (mL)	BF (min^{-1})	VT (mL)	head	TB	P	total	head	TB	P	total	head	TB	P	total
children	1484	25	19	303	6.93	5.15	7.51	19.59	43.66	7.04	19.33	70.03	87.36	6.71	3.10	97.17
adults	3122	50	16	625	10.35	5.09	6.48	21.92	58.59	5.68	15.04	79.31	92.13	3.50	1.97	97.60
the elderly	3402	50	16	625	10.38	5.06	6.00	21.44	58.93	5.73	14.17	78.83	92.23	3.41	1.94	97.58
males	3122	50	16	625	10.35	5.09	6.48	21.92	58.59	5.68	15.04	79.31	92.13	3.50	1.97	97.60
females	2468	50	16	625	10.28	5.16	7.67	23.11	57.76	5.58	17.13	80.47	91.85	3.87	1.91	97.63
general	2795	50	16	625	10.32	5.12	7.05	22.49	58.18	5.63	16.08	79.89	91.99	3.65	1.97	97.61

[a]Abbreviations: FRC: functional residual capacity; URT: upper respiratory tract; BF: breathing frequency; VT: tidal volume; TB: tracheobronchial region; P: pulmonary region.

MATERIALS AND METHODS

Study Design and Data Collection. The process of determining estimation error from the choices of dosimetry estimation consists of three steps. In step 1, the multiple-path particle dosimetry (MPPD) model was used to estimate the fractions of PM deposited in different regions in human airways. In step 2, we determined the relative mortality risk attributable to a 10 $\mu g/m^3$ increase in deposited PM using a two-stage statistical model.[5,21] Based on the established nationwide associations in step 2, the attributable mortality counts (MCs) from PM_1, PM with aerodynamic diameter between 1 and 2.5 μm ($PM_{1-2.5}$), and $PM_{2.5-10}$ were calculated in step 3. By presenting the dosimetry estimation in PM_1, $PM_{1-2.5}$, $PM_{2.5-10}$, $PM_{2.5}$, and PM_{10}, these three steps were iterated to compare dosimetry estimation-based mortality risk.

In this study, four types of data were required: daily air pollutants, daily mortality data, daily meteorological conditions, and population information. With the exception of PM_1 data, the daily concentrations of PM_1 data, the daily concentrations of $PM_{2.5}$, PM_{10}, NO_2, SO_2, O_3, and CO were obtained by averaging hourly measurements in each city.[5] With respect to PM_1, we first obtained the monthly averaged levels from satellite-derived PM_1 concentrations for each city from a previous study.[22] This previous study used a space-time extremely randomized tree model to derive PM_1 mass concentration at 1 km resolution.[22] Compared to other studies, the performance of the STET model is superior, as exemplified by the average cross-validation coefficient of determination of up to 0.77, combined with a relatively low root-mean-square error.[22] Then, the city-specific monthly average ratio of PM_1 to $PM_{2.5}$ was estimated. Further, the city-specific daily PM_1 concentrations were calculated by multiplying monthly $PM_1/PM_{2.5}$ ratio and the corresponding daily $PM_{2.5}$ levels. Daily mortality data were requested from 605 Chinese Disease Surveillance Points.[23] We clustered mortality data according to the 10th revision of the International Classification of Diseases[24] as follows: non-accidental causes (briefed as "all-cause", codes A00−R99), coronary heart disease ("CHD", codes I20−I25), cardiovascular disease ("CVD", codes I00−I99), stroke (codes I60−I69), chronic obstructive pulmonary disease ("COPD", codes J41−J44), and respiratory diseases ("RD", codes J00−J98). More detailed information on mortality data, as well as meteorological conditions, can be found in our previous reports.[5,20] The population information was derived from the statistical yearbook for each city. In total, 205 cities were selected due to data availability in the study period of 2014−2017, as illustrated in Supporting Information (SI) Figures S1 and S2.

Multiple-Path Particle Dosimetry (MPPD) Model. To estimate the deposition of PM in each region of the human respiratory tract (head region, TB region, and pulmonary region), the MPPD model (Version 3.04) was employed.[25] The MPPD model is capable of estimating the deposition fraction of PM in human airways and has been widely applied to assess risks to human health.[19,26,27] The stochastic module was chosen to estimate deposition patterns as utilized previously.[27,28] To run this model, input parameters include: (1) PM characteristics (diameter, shape, and density); (2) breathing parameters (tidal volume (TV, mL), and breathing frequency (BF, min^{-1})); (3) lung parameters (functional residual capacity (FRC) volume (mL), upper respiratory tract (URT) volume (mL)); and (4) exposure conditions (body orientation, inspiratory fraction, and breathing scenario). Based on the size distribution of Chinese cities summarized previously,[29−32] the median mass-adjusted diameters of PM_1, $PM_{1-2.5}$, and $PM_{2.5-10}$ were estimated to be 577, 1885, and 6181 nm, respectively. The density setting was 1.5 g/cm^3 for PM_1, 2 g/cm^3 for $PM_{1-2.5}$, and 1.7 g/cm^3 for $PM_{2.5-10}$, respectively.[33] The BF values of Chinese adults and children were obtained from a previous research.[34] URT volume and TV were set according to the International Commission on Radiological Protection and model recommendations,[35] and the FRC was calculated based on the following equations:[36]

for children

$$\text{male: FRC (mL)} = 0.125 \times 10^{-3} \times \text{height (cm)}^{3.298} \quad (1)$$

$$\text{female: FRC (mL)} = 0.286 \times 10^{-3} \times \text{height (cm)}^{3.136} \quad (2)$$

for adults and the elderly

$$\text{male: FRC (L)} = 2.34 \times \text{height (m)} + 0.01 \times \text{age (years)} - 1.09 \quad (3)$$

$$\text{female: FRC (L)} = 2.24 \times \text{height (m)} + 0.001 \times \text{age (years)} - 1.00 \quad (4)$$

Breathing path was assumed to be via the nose. Other model options were given as defaults. The parameters adopted in the MPPD model are summarized in Tables 1 and S1.

After obtaining the fractions of deposited PM_1, $PM_{1-2.5}$, and $PM_{2.5-10}$ for different population groups, the total deposition of PM (PM_T) was estimated as follows:

https://dx.doi.org/10.1021/acs.est.0c05095
Environ. Sci. Technol. 2021, 55, 1110−1121

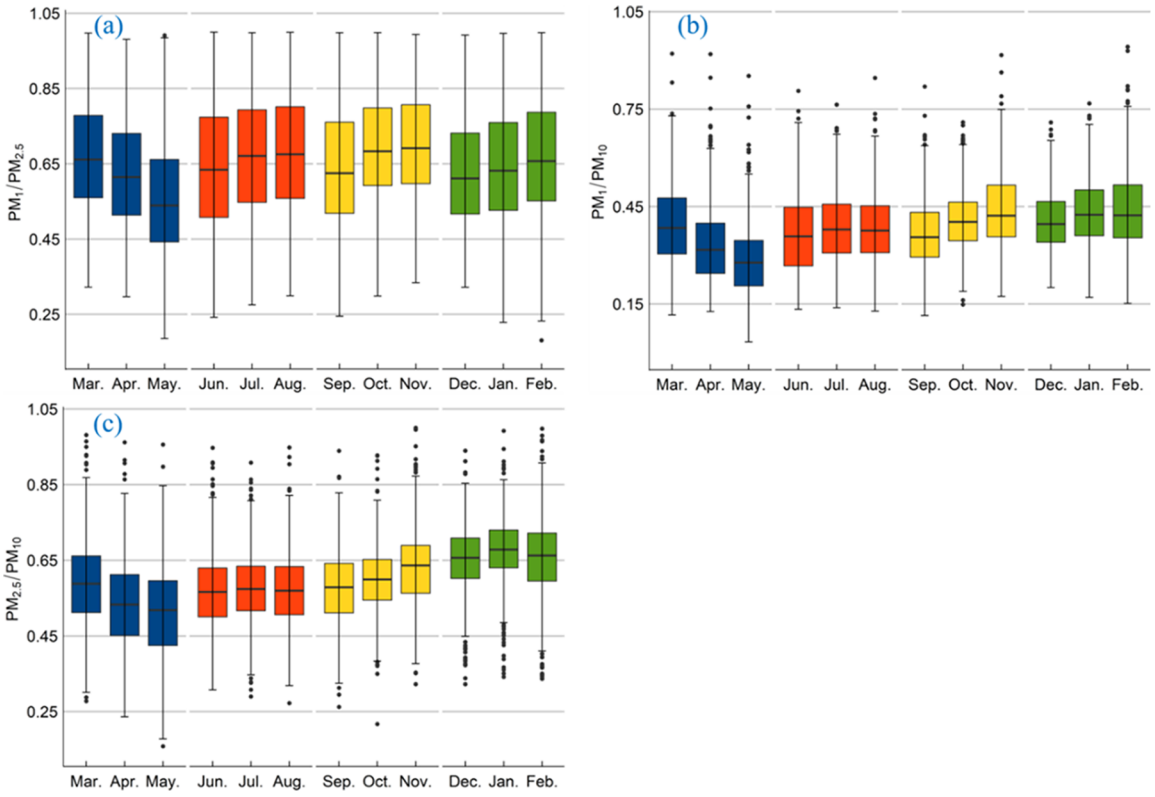

Figure 1. Monthly average ratio between PM_1, $PM_{2.5}$, and PM_{10} in 205 cities, China.

$$PM_T = \sum_{k=1}^{3} (PM_k \times F_{ij}) \tag{5}$$

where subscripts i and j represent the regions (head, TB, and P) of human airways and the different population groups (children, adults, the elderly, males, females, and general), respectively; F is the deposited fractions as estimated by MPPD model; and k (1, 2, 3) represents the three sizes of PM compositions, including PM_1, $PM_{1-2.5}$, and $PM_{2.5-10}$.

Statistical Analysis. To obtain the nationwide mortality risk attributable to size-fractioned PM, a two-stage statistical method was used.[1,5] In the first stage, a standard time-series regression model was applied to estimate city-specific associations between mortality and PM deposited concentration. The PM deposited concentration was defined as the sum of the product of each size-fraction PM concentration and the corresponding deposited fraction (5). In the MPPD model, the head regions include mouth cavity and nasopharyngeal passages.[37] Most PM deposited in this area can be removed by a range of activities, such as breathing through the nasopharynx, passages and mouth breathing, coughing, and others,[38] and thus the deposited dose reaching the deep-lying systems (such as TB and pulmonary region) is particularly concerned.[39,40] Thus, in this study, the sum deposited concentration in TB and pulmonary regions was used for nonaccidental causes. The deposited PM mass concentrations in TB and pulmonary regions were treated as independent factors for respiratory and circulatory system diseases, respectively.

With respect to time-series analysis, the incidence of mortality was assumed to a Poisson distribution with a parameter of μ (6) to avoid overdispersion. Then, a natural spline smooth function (nssf) of calendar day was applied to account for the long-term temporal trends in mortality, and the degree of freedom (df) was assumed to be 7 according to prior studies.[1,4] After that, day of the week (dow) was included as a confounding variable to control for short-term weekly variations.[20] Finally, the 3-day moving averages of temperature (temp) and relative humidity (rh) with 3 df were also considered as confounding variables, since previous studies revealed these two factors may influence mortalities[5,41]

$$mortality \sim Poisson(\mu)$$
$$\log(\mu) \sim PM_{2.5} + ns\_date + dow + temp + rh \tag{6}$$

After obtaining the city-specific coefficient in the first stage, we conducted a meta-analysis to pool the city-specific associations into a nationwide estimate in the second stage.[42] A standard meta-analysis process was applied,[43] using the package of metafor in R. In addition, stratified analysis by geography, seasons (warm period: May to October; cold period: November to April), and demographic factors (age (5−64, 65−75, and ≥75 years), sex, and education) was performed to elucidate the potential effects between subgroups. In particular, the effects of PM pollution on mortality were not estimated for children, considering the mortality rate for children was much lower than for adults and the elderly.

Estimation of National Deaths. To evaluate the nonaccidental mortality risk associated with PM exposure, we first calculated attributable fractions (AF) due to PM_1, $PM_{1-2.5}$, and $PM_{2.5-10}$ as follows[44,45]

$$AF_{ij} = \frac{\exp^{(\beta_i \times (TB_{ij} + P_{ij})/10)} - 1}{\exp^{(\beta_i \times (TB_{ij} + P_{ij})/10)}} \tag{7}$$

where TB and P are the PM deposited concentration in the TB and pulmonary regions ($\mu g/m^3$), β is the estimated coefficient

https://dx.doi.org/10.1021/acs.est.0c05095
Environ. Sci. Technol. 2021, 55, 1110−1121

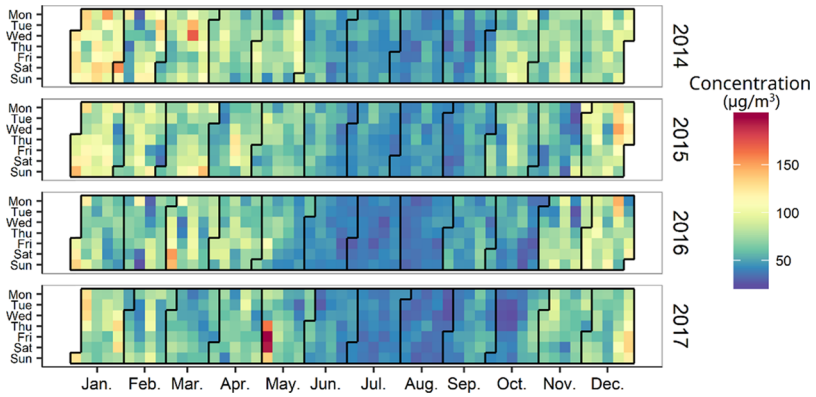

Figure 2. Daily average concentration of total deposited particulate matter in head, tracheobronchial, and pulmonary regions with the population weight during 2014−2017, China.

of daily mortality per 10 $\mu g/m^3$ increase obtained from the meta-analysis, i is the particular subgroup indexed by demographical factors, and j represents the city.

Similarly, with respect to mortality risk of RD and COPD, AF was expressed as

$$AF_{ij} = \frac{\exp^{(\beta_i \times TB_{ij}/10)} - 1}{\exp^{(\beta_i \times TB_{ij}/10)}} \quad (8)$$

Regarding the estimation for CVD, CHD, and stroke deaths, AF was written as

$$AF_{ij} = \frac{\exp^{(\beta_i \times P_{ij}/10)} - 1}{\exp^{(\beta_i \times P_{ij}/10)}} \quad (9)$$

For each city (j), the mortality counts (MC) of the particular subgroups (i) were calculated by multiplying the corresponding city-specific AF, city-specific mortality (M), and the city population (POPU)

$$MC_{ij} = AF_{ij} \times M_{ij} \times POPU_{ij} \quad (10)$$

Sensitivity Analysis. Two types of sensitivity analyses were performed. First, this study used 577, 1885, and 6181 nm to represent the median mass-adjusted size of PM_1, $PM_{1-2.5}$, and $PM_{2.5-10}$, respectively. To test the influence of these settings on the estimation of mortality risk, we scaled up the adopted median sizes in the range of −20 to 20% and conducted our main analyses again. The second type of sensitivity analysis was carried out by altering the parameter settings, including the outdoor air temperature, relative humidity, degrees of freedom in calendar year, and lag patterns of the dose metric, as detailed in our earlier studies.[4,5,20]

RESULTS

Descriptive Statistics. The statistics of size-fractioned PM in 2014−2017 are tabulated in Table S2. In particular, the nationwide PM_1, $PM_{2.5}$, and PM_{10} levels were 33 ± 21, 54 ± 42, and 93 ± 63 $\mu g/m^3$, respectively. Figure 1 summarizes the monthly ratio between PM_1, $PM_{2.5}$, and PM_{10} during the study period. The monthly averaged ratios of PM_1/PM_{10} and $PM_{2.5}/PM_{10}$ were 0.39 ± 0.12 and 0.59 ± 0.11, respectively. Moreover, the proportion between PM_1 and $PM_{2.5}$ was estimated to be 0.65 ± 0.16, which was in the range reported previously.[8,46] With respect to seasonal variability, the $PM_1/PM_{2.5}$, PM_1/PM_{10}, and $PM_{2.5}/PM_{10}$ ratios were the highest in autumn, winter, and winter, respectively, while the lowest ratios for $PM_1/PM_{2.5}$, PM_1/PM_{10}, and $PM_{2.5}/PM_{10}$ were all observed in the spring. Over the course of the study period, there were an average 18.7 ± 19.4 nonaccidental deaths per day in the 205 surveyed cities.

Characteristics of PM Deposition in the Human Body. Using the MPPD model and parameters presented in Tables 1 and S1, we estimated the fraction of deposited PM (Table 1). Overall, more than 85% of inhaled coarse PM was deposited in the head region (87.36−92.23%), followed by the TB region (3.41−6.71%) and pulmonary region (1.91−3.1%), indicating that coarse PM is less likely to deposit in the deeper respiratory tract and pulmonary alveoli. In contrast, the fraction of $PM_{1-2.5}$ in the head decreased to the range of 43.66−58.93% and the fractions of $PM_{1-2.5}$ in TB and P increased to 5.58−7.04 and 14.17−19.33%, respectively. The total deposition fraction of PM_1 was 19.59−23.11%, which was about 72% lower than that of $PM_{1-2.5}$ and 78% lower than that of coarse PM. The deposition order of PM_1 was similar to that of $PM_{1-2.5}$, with the maximum in the head region (6.93−10.38%), followed by the pulmonary region (6.00−7.67%) and the TB region (5.06−5.16%).

The disparities of depositions between age groups are reported in Table 1. Though with the lowest total deposition percentage, children exhibited a higher deposition percentage in the pulmonary region than in other subgroups. A negligible difference between adult and elderly groups was noted (Table 1). With respect to gender variability, a higher fraction of deposition in the pulmonary region was observed for PM_1 and $PM_{1-2.5}$ in females, while the differences were much lower for deposition in other airway regions between males and females (Table 1).

Together with 5 and the parameters tabulated in Table 1, we estimated the daily averaged concentration of PM deposited in the general population (Figure S3). As shown, significantly higher deposited PM occurred in the cold season rather than the warm season. Particularly, the deposited PM in the winter was 81 ± 23 $\mu g/m^3$, which is 85% higher than the 44 ± 8 $\mu g/m^3$ deposited in the summer. The annual deposited PMs in 2014, 2015, 2016, and 2017 were estimated to be 69 ± 49, 64 ± 46, 58 ± 44, and 58 ± 48 $\mu g/m^3$, respectively, indicating a decreasing trend of 3.7 ± 3.2 $\mu g/m^3$ per year. The temporal trend of PM deposited was also estimated using population weight in each city (Figure 2): the deposited PMs in winter and summer were determined to be 84 ± 25 and 45 ± 9 $\mu g/m^3$, respectively, which were close to the estimation without the consideration of population weight. The concentrations of

https://dx.doi.org/10.1021/acs.est.0c05095
Environ. Sci. Technol. 2021, 55, 1110−1121

total deposited PM without population weight in 205 cities are also provided in Figure S4, and the annual and seasonal maps on the spatial distribution for PM_1, $PM_{1-2.5}$, and $PM_{2.5-10}$ are provided in SI Figures S5−S11. Among the 205 cities, the highest deposited PM levels were observed in central and northeastern China, while lower levels were found in southern China.

Associations between PM Deposition and Daily Mortality. Overall, each 10 $\mu g/m^3$ increase in deposited PM was significantly associated with a nationwide increment of 1.12% (95% confidence interval (CI), 0.77−1.49%) in all-cause mortality (Table 2). For cause-specific mortality, the pooled estimation per 10 $\mu g/m^3$ increment in deposited PM was 1.86% (95% CI, 1.17−2.56%) for CVD, 1.61% (95% CI, 0.72−2.51%) for CHD, 1.68% (95% CI, 0.85−2.52%) for stroke, 4.64% (95% CI, 2.74−6.58%) for RD, and 5.74% (95% CI, 3.52−8.00%) for COPD (Table 2). Additionally, we found regional heterogeneity in the associations between PM exposure and daily mortality. For example, the effect of deposited PM on all-cause or most cause-specific mortality in the southern regions was approximately 2-fold higher than the effects in northern regions (Table 2), which may be explained by the relatively lower pollution of PM and potential demographic vulnerability in southern regions.[46,47] With respect to seasonal differences, our finding suggested that the effect of PM on COPD risk in the warm season was 8.02% (95% CI, 2.79−13.50%), whereas a weaker effect (5.81% with 95% CI of 3.29−8.39%) was determined in the cold season. Except for COPD, the seasonal difference in the associations between PM and other causes of mortality was not significant. The higher effects in COPD mortality in the warm period may be associated with the relatively lower PM pollution in the warm season. In addition, people usually have more outdoor activities in the warm season.[48,49]

Regarding demographic factors, the strongest associations between PM exposure and most cause-specific mortality were found in the elderly due to population vulnerability. Compared to females, significantly higher effects were determined in males. Additionally, higher effects for nonaccidental mortality in the low educational population were observed. Our findings concerning age and gender differences in the PM-associated effects (Table 2) are in accordance with the findings from the majority of previous studies.[4,5,20]

Attributable Fractions and Mortality Counts of Cause-Specific Deaths. We used 8−11 to estimate AF and mortality counts of PM-associated deaths, as summarized in Table 3. The estimate of AF caused by $PM_{1-2.5}$ was 0.48% (95% CI, 0.33−0.64%), followed by PM_1 (0.45% with 95% CI of 0.30−0.59%) and $PM_{2.5-10}$ (0.24% with 95% CI of 0.16−0.31%). The total MC attributable to short-term exposure to PM exposure was 99 826 cases per year. In particular, the estimates of MC (in cases per year) were 42 603 (95% CI: 29 219−56 617) for $PM_{1-2.5}$, 37 214 (95% CI: 25 438−49 469) for PM_1, and 19 009 (95% CI: 12 990−25 278) for coarse PM. Individual estimates of MC and AF at city scale are plotted in Figures 3 and S12, respectively, and the regional, seasonal, and demographical estimations on AF and MC are also tabulated in Table 3. Among the 205 cities, those with a higher MC were observed in central and southwestern China, including Shandong, Henan, Hebei, Beijing, Tianjin, and Chongqing, which have large populations and severe PM pollution. For example, the city with the highest MC was Chongqing Municipality (2328 cases per year) due to a

Table 2. National, Regional, Seasonal, and Demographic Average Relative Risk (95% Confidence Interval, Unit: %) in Daily Cause-Specific Mortality per 10 $\mu g/m^3$ Increase in 2-Day Moving Average Particulate Matter Deposited in the Human Airways[a]

		estimates					
characteristic	level	all-cause	CVD	CHD	stroke	RD	COPD
region	north	0.81 (0.39−1.24)	1.13 (0.35−1.91)	0.94 (−0.07−1.96)	1.04 (0.10−2.00)	3.92 (1.78−6.11)	6.01 (3.48−8.60)
	south	1.61 (0.98−2.24)	3.28 (2.03−4.54)	3.73 (1.97−5.52)	2.92 (1.41−4.46)	5.64 (2.29−9.11)	4.93 (1.09−8.92)
seasons	cold	1.11 (0.72−1.5)	1.97 (1.20−2.75)	1.96 (1.01−2.93)	1.70 (0.70−2.70)	5.17 (2.95−7.45)	5.81 (3.29−8.39)
	warm	1.04 (0.37−1.73)	1.88 (0.33−3.45)	1.25 (−0.70−3.23)	2.01 (0.20−3.86)	5.13 (0.34−10.1)	8.02 (2.79−13.50)
gender	male	1.05 (0.62−1.49)	2.02 (1.12−2.93)	1.68 (0.36−3.03)	1.78 (0.82−2.75)	4.67 (2.44−6.96)	6.19 (3.52−8.94)
	female	1.11 (0.69−1.52)	1.57 (0.80−2.35)	1.47 (0.52−2.43)	1.36 (0.39−2.33)	5.10 (2.37−7.90)	4.84 (1.72−8.06)
age	5−64 years	0.73 (0.25−1.22)	1.47 (0.35−2.62)	1.29 (−0.79−3.40)	1.36 (−0.11−2.86)	5.51 (−0.93−12.40)	2.17 (−6.98−12.20)
	65−74 years	0.78 (0.20−1.37)	1.04 (−0.19−2.30)	1.96 (0.149−3.80)	0.35 (−1.48−2.20)	5.57 (0.71−10.70)	7.57 (1.89−13.60)
	≥75 years	1.50 (1.04−1.96)	2.67 (1.70−3.65)	2.16 (0.89−3.44)	2.83 (1.54−4.13)	5.60 (3.02−8.24)	6.56 (3.66−9.53)
education	>9 years	0.79 (−0.08−1.67)	2.25 (0.14−4.40)	3.45 (0.68−6.29)	−0.02 (−3.07−3.12)	−3.15 (−10.80−5.19)	−5.40 (−19.10−10.60)
	≤9 years	1.16 (0.78−1.53)	1.88 (1.16−2.61)	1.67 (0.74−2.61)	1.76 (0.90−2.63)	5.05 (3.03−7.11)	5.76 (3.44−8.13)
combined	all	1.12 (0.77−1.49)	1.86 (1.17−2.56)	1.61 (0.72−2.51)	1.68 (0.85−2.52)	4.64 (2.74−6.58)	5.74 (3.52−8.00)

[a]Abbreviations: all-cause: nonaccidental causes; CVD: cardiovascular diseases; CHD: coronary heart disease; RD: respiratory disease; COPD: chronic obstructive pulmonary disease.

https://dx.doi.org/10.1021/acs.est.0c05095
Environ. Sci. Technol. 2021, 55, 1110−1121

Table 3. Attributable Fractions and Mortality Counts of Cause-Specific Deaths (95% Confidence Interval) due to Short-Term Exposure to Size-Fractioned Particulate Matter in China[a]

causes and subgroups		attributable fraction (%)			mortality counts (cases/year)		
		PM_1	$PM_{1-2.5}$	$PM_{2.5-10}$	PM_1	$PM_{1-2.5}$	$PM_{2.5-10}$
all-cause		0.45 (0.30, 0.59)	0.48 (0.33, 0.64)	0.24 (0.16, 0.31)	37 214 (25 438, 49 469)	42 603 (29 129, 56 617)	19 009 (12 990, 25 278)
gender	female	0.47 (0.29, 0.64)	0.50 (0.31, 0.69)	0.24 (0.15, 0.33)	16 657 (10 424, 22 789)	18 947 (11 861, 25 913)	8306 (5196, 11 368)
	male	0.40 (0.23, 0.56)	0.43 (0.26, 0.61)	0.21 (0.13, 0.30)	18 962 (11 170, 26 884)	21 772 (12 829, 30 858)	9911 (5836, 14 057)
age	5−64 years	0.28 (0.09, 0.46)	0.30 (0.10, 0.50)	0.15 (0.05, 0.25)	5524 (1858, 9236)	6335 (2132, 10 587)	2909 (978, 4865)
	65−74 years	0.28 (0.07, 0.50)	0.31 (0.08, 0.54)	0.16 (0.04, 0.27)	5130 (1315, 8988)	6041 (1549, 10 581)	2783 (713, 4878)
	≥75 years	0.54 (0.38, 0.71)	0.59 (0.41, 0.77)	0.30 (0.21, 0.39)	24 244 (16824, 31 650)	27 805 (19 301, 36 288)	12 853 (8916, 16 786)
region	south	0.60 (0.36, 0.84)	0.60 (0.36, 0.83)	0.25 (0.15, 0.35)	25 767 (15 703, 35 806)	26 105 (15 912, 36 271)	10 669 (6498, 14 836)
	north	0.35 (0.17, 0.53)	0.41 (0.20, 0.62)	0.22 (0.10, 0.33)	14 017 (6757, 21 332)	17 769 (8569, 27 029)	8423 (4059, 12 823)
CVD		0.43 (0.27, 0.59)	0.59 (0.37, 0.82)	0.14 (0.09, 0.19)	17 957 (11 306, 24 694)	27 008 (17 015, 37 115)	5692 (3581, 7831)
CHD		0.37 (0.17, 0.58)	0.51 (0.23, 0.80)	0.12 (0.05, 0.18)	6149 (2734, 9575)	9361 (4166, 14 564)	1991 (885, 3103)
stroke		0.39 (0.20, 0.58)	0.54 (0.27, 0.80)	0.12 (0.06, 0.19)	7852 (3986, 11 766)	11 688 (5938, 17 500)	2450 (1243, 3674)
COPD		0.96 (0.59, 1.33)	0.64 (0.39, 0.89)	0.78 (0.48, 1.09)	7325 (4501, 10 189)	5035 (3092, 7006)	5552 (3410, 7725)
RD		0.78 (0.46, 1.10)	0.52 (0.31, 0.74)	0.63 (0.37, 0.90)	7770 (4596, 11 000)	5282 (3123, 7480)	5870 (3471, 8313)

[a]Abbreviations: all-cause: nonaccidental causes; CVD: cardiovascular diseases; CHD: coronary heart disease; RD: respiratory disease; COPD: chronic obstructive pulmonary disease; PM_{0-1}: particulate matter with an aerodynamic diameter less than 1 μm; $PM_{1-2.5}$: particulate matter with an aerodynamic diameter between 1 and 2.5 μm; $PM_{2.5-10}$: particulate matter with an aerodynamic diameter between 2.5 and 10 μm.

https://dx.doi.org/10.1021/acs.est.0c05095
Environ. Sci. Technol. 2021, 55, 1110−1121

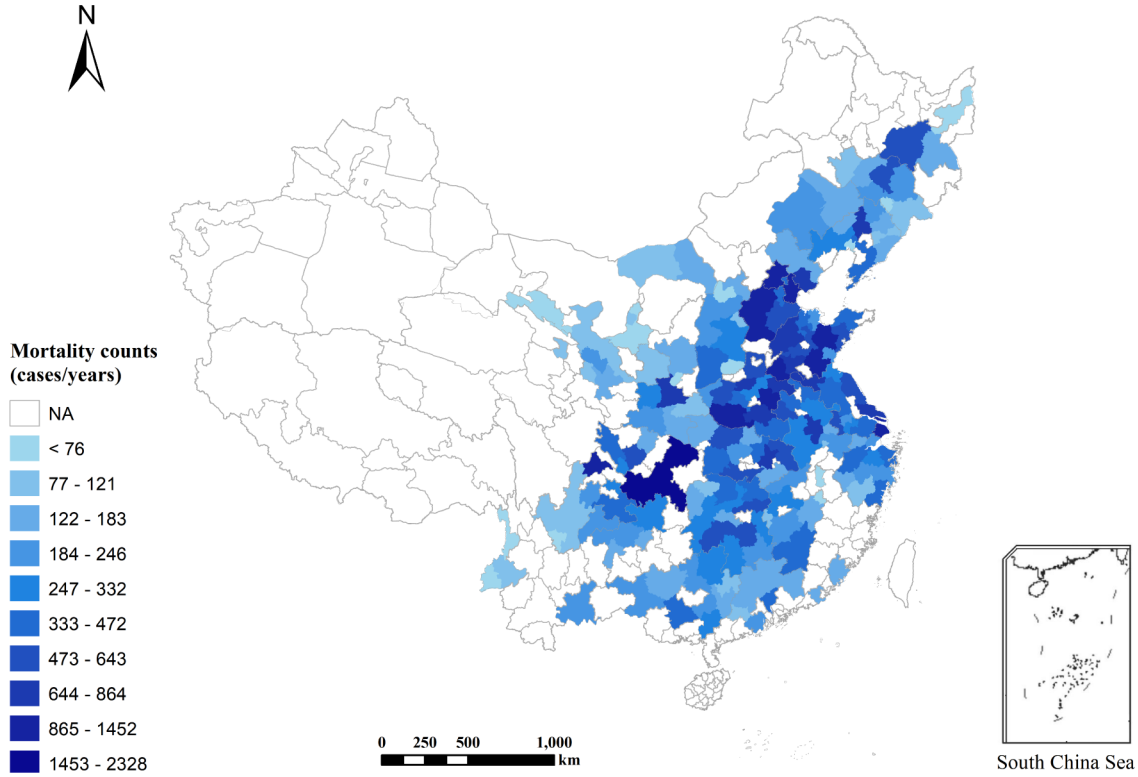

Figure 3. Spatial distributions of annual average mortality count attributable to short-term exposure to total deposited particulate matter for 205 cities, China. NA: not available.

Table 4. Estimation of Mortality Counts (95% Confidence Interval) Based on Different Choices of Dosimetry Estimation in China (Unit: 10 000 Cases Per Year)

	all-cause	CVD	CHD	Stroke	RD	COPD
PM_1	9.55 (6.62, 12.43)	5.14 (3.38, 6.90)	1.99 (1.01, 2.97)	2.14 (1.05, 3.22)	1.86 (1.13, 2.59)	1.65 (1.01, 2.29)
$PM_{2.5}$	8.89 (5.95, 11.82)	4.96 (3.18, 6.73)	1.80 (0.85, 2.75)	2.08 (1.03, 3.11)	1.54 (0.84, 2.24)	1.47 (0.86, 2.09)
PM_{10}	11.41 (8.08, 14.66)	6.42 (4.34, 8.45)	2.28 (1.21, 3.36)	2.92 (1.70, 4.13)	1.88 (1.14, 2.61)	1.75 (1.10, 2.39)
$PM_{2.5-10}$	7.79 (5.12, 10.44)	4.40 (2.66, 6.12)	1.52 (0.64, 2.41)	2.20 (1.25, 3.15)	1.24 (0.61, 1.86)	1.14 (0.60, 1.67)
$PM_{1-2.5}$	4.96 (2.51, 7.39)	3.06 (1.51, 4.59)	0.97 (0.20, 1.74)	1.33 (0.51, 2.15)	0.74 (0.16, 1.32)	0.84 (0.30, 1.38)
size-combined PM	9.88 (6.76, 13.14)	5.07 (3.19, 6.96)	1.75 (0.78, 2.72)	2.20 (1.12, 3.29)	1.79 (1.10, 2.49)	1.89 (1.12, 2.68)

[a]Abbreviations: all-cause: nonaccidental causes; CVD: cardiovascular diseases; CHD: coronary heart disease; RD: respiratory disease; COPD: chronic obstructive pulmonary disease; PM_1: particulate matter with an aerodynamic diameter less than or equal to 1 μm; $PM_{2.5}$: particulate matter with an aerodynamic diameter less than or equal to 2.5 μm; PM_{10}: particulate matter with an aerodynamic diameter less than or equal to 10 μm; $PM_{1-2.5}$: particulate matter with an aerodynamic diameter between 1 and 2.5 μm; $PM_{2.5-10}$: particulate matter with an aerodynamic diameter between 2.5 and 10 μm.

permanent population of over 31 million and severe long-term PM pollution caused by a valley terrain and poor atmospheric diffusion conditions. In contrast, cities with lower recorded MC in northwestern and southern China, such as Yunnan, Gansu, Ningxia, southern Sichuan, and Guangdong provinces, had relatively better air quality and lower population. Actually, the PM concentration contributed approximately 15.4% to the spatial difference in MC. For cause-specific mortality, $PM_{1-2.5}$ accounted for most cardiovascular mortality and PM_1 was the driving factor for respiratory mortality.

Figure S13 indicates that a change in size used in the MPPD model slightly altered the estimation on mortality counts, and the use of alternative conditions for outdoor humidity, temperature, and calendar years slightly influenced the results (Figures S14−S16). The choices of lag patterns of dose metric could moderately modify the mortality counts (Figure S17).

Comparison of the Mortality Risks for Different Exposure Metric. In our study, we also recalculated the determination of PM-associated mortality risk using direct dosimetry estimations rather than deposition fraction. Table S3 illustrates that the excess risk of daily mortality per 10 $\mu g/m^3$ increment varied between different dose metrics: 0.35% (95% CI, 0.24−0.46%) for PM_1, 0.28% (95% CI, 0.14−0.42%) for $PM_{1-2.5}$, 0.20% (95% CI, 0.13−0.27%) for $PM_{2.5}$, 0.26% (95% CI, 0.17−0.35%) for $PM_{2.5-10}$, 0.15% (95% CI, 0.11−0.20%) for PM_{10}, and 1.12% (95% CI, 0.77−1.49%) for size-combined PM. The corresponding estimates of AF were 1.16% (95% CI, 0.80−1.51%), 0.57% (95% CI, 0.2−0.85%), 1.05% (95% CI, 0.70−1.41%), 0.97% (95% CI, 0.64−1.31%), 1.39% (95% CI, 0.98−1.79%), and 1.17% (95% CI, 0.80−1.55%), respectively (Table S4). Furthermore, we calculated the mortality counts when using different dose metrics (Table 4). The results from the use of PM_1 and $PM_{2.5}$ were similar to that based on size-

https://dx.doi.org/10.1021/acs.est.0c05095
Environ. Sci. Technol. 2021, 55, 1110−1121

combined PM. However, using PM_{10} may overestimate the MCs, whereas the choices of coarse PM and $PM_{1-2.5}$ resulted in underestimations.

DISCUSSION

The mortality risk caused by PM exposure poses a significant public concern, and yet the estimation error associated with the choices of dosimetry estimations remains unclear. Our study first indicated the use of PM_1, $PM_{2.5}$, PM_{10}, coarse PM, or deposited PM as dose metric triggered a different mortality risk (Table S3), but the estimated total MCs were less differentiated (Table 4). A similar result was also reported when comparing the effects of total suspended particulate (TSP) and PM_{10} on life expectancy in China.[50,51] This prior report indicated that exposure to 100 $\mu g/m^3$ of TSP was associated with a reduction in life expectancy of about 3.0 years.[51] Given that the PM_{10} contributed to approximately 45.4% of TSP, this estimate expressed in a prediction that 10 $\mu g/m^3$ of PM_{10} was about 0.66 years (3.0/100*10/45.4% = 0.66 years), which is in accordance with the estimation of 0.64 years using PM_{10} as dose metric.[50] Also, based on 652 cities, worldwide estimations of 0.44 and 0.68% excess mortality risk were determined for 10 $\mu g/m^3$ uptick in PM_{10} and $PM_{2.5}$,[1] respectively, which may be attributable to an approximate ratio of 0.6 between $PM_{2.5}$ and PM_{10}.

In line with these studies, we found that the gap of total MCs resulted from most dose metrics was in a narrow range (Table 4). While our study demonstrated that the estimated risk based on PM_x was close to that based on total deposited PM, the results of some previous reports using PM_x as dose metric may indicate that estimated risk was mainly or totally caused by PM_x rather than total PM. Thus, these studies may exaggerate the "true" effect of PM_x at least to some extent. When exploring the PM_x-associated mortality effect, most studies did not consider the collinearities between different sizes of PM (Figure S18), although including such collinearities in the analysis may significantly lower the effects.

On another aspect, although most estimations on mortality counts were similar, some disparities were still determined (Table 4), and we speculated that these disparities may be related to the coefficient of variation (CV) of the dosimetry estimations. To test this hypothesis, we examined the average CV of 205 selected cities and the estimated mortality counts. Negative correlations between the CV and mortality counts were found (Figure 4), demonstrating that increased CV markedly lowers the mortality counts. Such appearance may be explained by the weighting of dose metrics with smaller CVs, which were larger in the regression and thus triggered a large slope.

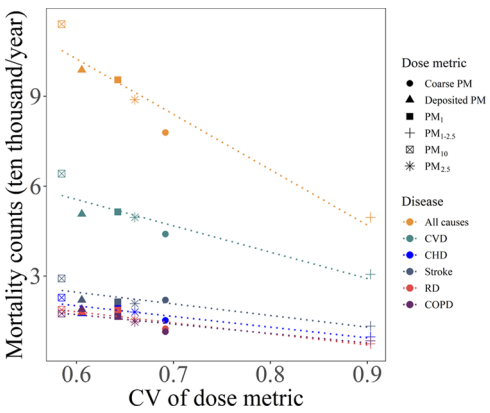

Figure 4. Correlations between coefficients of variation (CV) of dose metric and mortality counts.

To further validate our hypothesis, we chose $PM_{2.5}$ as a case study by altering $PM_{2.5}$ on day j in city i with a scale factor of λ as follows:

$$P = PM_{2.5-ij} + \lambda \times (PM_{2.5-ij} - mean(PM_{2.5-i})) \quad (12)$$

where P is the new dose metric. One merit of this treatment is that only the CV was changed while the average value of $PM_{2.5}$ remained unchanged, which can exclude the influence of the difference in the average levels of $PM_{2.5}$. The λ value was set in a range of −30 to 30%, indicating that the CV of $PM_{2.5}$ was scaled from 70 to 130%. As illustrated in Figure S19, a negative trend between the CV and coefficient was noted, supporting our earlier proposition.

Previous studies have utilized various dose metrics to link the mortality and PM exposure. As reported in prior nationwide analyses, each 10 $\mu g/m^3$ uptick in $PM_{2.5}$ and $PM_{2.5-10}$ was significantly associated with increments of 0.22 and 0.23%, respectively, in nonaccidental causes of mortality in 272 Chinese cities.[4,20] A meta-analysis concluded that a 10 $\mu g/m^3$ increase in $PM_{2.5}$ and PM_{10} is linked with 0.40 and 0.36% increases in nonaccidental mortality in China, respectively.[47] Our results using $PM_{2.5}$ and $PM_{2.5-10}$ as dosimetry estimations were in these ranges. However, caution should be raised before interpreting that the effects were all or majorly caused by PM_x, since most available reports did not examine the potential effects from other sizes of PM. Directly integrating other sizes of PM as confounding variables may be a poor option, given that the PM deposition in human airways varied considerably between different sizes of PM.[17]

Therefore, applying the MPPD model in epidemiological studies seems a promising approach. The MPPD model established for laboratory species and human has gone through many years of developments and validations,[37,52] and is currently widely used by researchers and regulatory organizations to predict the deposition of PMs in the human respiratory tract.[18,28,40,53] In particular, this mechanistic model calculates the deposition utilizing theoretically derived efficiencies for deposition by diffusion, sedimentation, and impaction within the airway or airway bifurcation.[17] However, it should be noted that there are also some limitations to this model. For example, the MPPD model does not consider the interaction between PMs, which may influence the PM deposition in human airways.

Modeling studies revealed that three mechanisms control PM deposition in the human lung: inertial impaction, gravitational sedimentation, and Brownian diffusion.[17] As the size of the PM decreased, the region of PM deposition moved from the upper airway to deeper pulmonary regions based on different dominant mechanisms. Particularly, inertial impaction is the major factor for $PM_{2.5-10}$ deposited in the head region and URT, while $PM_{1-2.5}$ deposited in the deeper respiratory tract and the pulmonary region is mainly controlled by sedimentation and diffusion. Furthermore, the PM_1 deposition in the human airway is driven mainly by diffusion, resulting in a comparable deposition fraction in the TB region between $PM_{1-2.5}$ and PM_1. Furthermore, due to relatively higher levels of PM_1, deposited mass concentrations of PM_1 in TB were approximately 47% higher than that of $PM_{1-2.5}$, resulting in that PM_1 is the driving factor for respiratory mortality. More

https://dx.doi.org/10.1021/acs.est.0c05095
Environ. Sci. Technol. 2021, 55, 1110−1121

broadly, the MPPD model also demonstrates that $PM_{1-2.5}$ is prone to deposit in the pulmonary region by sedimentation,[17] which led to much higher deposited concentrations of $PM_{1-2.5}$ in the pulmonary region than other size-fractioned PM, triggering the highest contribution of $PM_{1-2.5}$ in circulatory diseases. Circulatory disease is also the primary factor for total mortality in China,[20] and therefore the contribution from $PM_{1-2.5}$ to total mortality was the highest.

Compared to other dose metrics, the estimations of deposited PM in human airways involve a few parameters. Furthermore, although our study demonstrated that the use of deposited PM may lead to incremental benefit in the projection of MCs, the use of deposited PM can broaden our knowledge in at least three aspects: (1) help explain the population variations in response to PM pollution; (2) highlight the importance of the toxicities of size-fractioned PMs; and (3) evaluate the contributions from different sizes of PMs to total MCs. Thus, our study reinforced the importance of the size of PM in relevant research.

Recently, studies on the adverse effects in relation to the smaller size of PM are increasing.[13,46,54,55] A very recent study also pointed out that the deposited rate of PM with a smaller size can be up to 50%.[40] Hence, deposition from a smaller size of PM is important to PM pollution. In our study, we used a zero threshold to estimate the PM-associated mortality, which aimed to compare our results to previous studies.[4,20] However, a threshold in the range of 2.4−7.5 $\mu g/m^3$ was also common in some existing dose−response curves to estimate the PM-associated risk.[56,57] Thus, we recalculated the mortality counts using a threshold of 5 $\mu g/m^3$ for $PM_{2.5}$, and the total mortality counts were estimated to be 81 042 (54 263−107 724), yielding an acceptance error with <10% difference (Table S5). However, the influence of the choices of threshold may be required for in-depth investigation in future, while prior studies have demonstrated that the PM-associated risk, in some cases, may be sensitive to the shape of concentration−response association.[58,59]

To date, PM_1 is not included in regular monitoring of pollution in China, and monitoring data of PM_1 are only available across about 90 cities. The monitoring PM_1 data indicated a slightly higher variability than that of $PM_{2.5}$. This study used the simulated PM_1 data from a previous report.[22] To validate the data quality of PM_1, the additional mortality risk in daily morality per 10 $\mu g/m^3$ increase of PM_1 for the overlapped cities was reestimated, which revealed relative differences within an acceptable baseline (less than 20%).

Some limitations should be noted. There was an underlying assumption that all size-fractioned PM has the same toxicity, which is in contrast to previous findings.[10] Actually, the variations in the components of PM can result in different toxicities of the size-fractioned PM. For example, some available studies indicated that black carbon (BC), a component of PM that tends to concentrate in a smaller size of PM,[60] can potentially trigger higher risk of PM_1 than that of PM_{10} or $PM_{2.5}$.[61,62] Thus, smaller-size PM may carry more toxin and exhibit higher toxicity,[63,64] which may underestimate the contribution of PM_1 on mortality but overestimate that from $PM_{1-2.5}$ and coarse PM. In addition, our study utilized a uniform median size to represent PM_1, $PM_{1-2.5}$, and $PM_{2.5-10}$ when determining nationwide PM deposition. While sensitivity analysis indicated limited influence from the alternatives of median size (Figure S13), the variations of size distributions between 205 regions may alter our results. Third, this study used the ambient PM as dose metric, although an estimation bias between ambient PM and the personal PM has been demonstrated.[65] Meanwhile, the seasonal difference in breathing parameters, outdoor activity patterns, and particle diameter among the 205 cities were not considered when calculating the deposited PM, which may also impact our estimation.

In summary, our study reinforced the evidence of a link between mortality and short-term exposure to PM and also determined the cause-specific mortality risk from various sizes of PM. The count of short-term exposure to PM deposition-associated mortality was determined as 99 826 cases/year in China, with major contributions from PM_1 and $PM_{1-2.5}$. This study also suggested that the disparities of the estimated mortality counts between the dose metric may be caused by its coefficient of variations. Given the potential collinearities between size-fractioned PM, the caution should be exercised when interpreting the mortality risk associated with PM_x.

■ ASSOCIATED CONTENT

Supporting Information

The Supporting Information is available free of charge at https://pubs.acs.org/doi/10.1021/acs.est.0c05095.

Administrative division and flowchart of 205 cities selected in this study; spatial distributions of annual average concentration of total deposited particulate; spatial distributions of attributable fractions of mortality risk due to particulate matter exposure; sensitivity analysis; correlation matrix between different sizes of particulate matter; relationships between scaled CV (coefficient of variation) and percentage differences in daily all-causes mortality per 10 $\mu g/m^3$ increment in $PM_{2.5}$; parameters defaulted by multiple-path particle dosimetry model; summary statistics of regional daily PM concentration; estimation of excess risk in daily cause-specific per 10 $\mu g/m^3$ increase in 2-day moving average concentration of different exposure metrics; estimation of attributable fraction based on different choices of dosimetry estimation; and sensitivity analysis for the setting of threshold (PDF)

■ AUTHOR INFORMATION

Corresponding Author

Zhaomin Dong − *School of Space and Environment and Beijing Advanced Innovation Center for Big Data-Based Precision Medicine, Beihang University, Beijing 100191, China;* orcid.org/0000-0002-0251-2355; Email: dongzm@buaa.edu.cn, chaomi_87@163.com

Authors

Hao Wang − *School of Space and Environment and Beijing Advanced Innovation Center for Big Data-Based Precision Medicine, Beihang University, Beijing 100191, China*

Peng Yin − *National Center for Chronic and Noncommunicable Disease Control and Prevention, Chinese Center for Disease Control and Prevention, Beijing 100050, China;* orcid.org/0000-0002-5515-2824

Wenhong Fan − *School of Space and Environment and Beijing Advanced Innovation Center for Big Data-Based Precision Medicine, Beihang University, Beijing 100191, China*

Ying Wang − *School of Space and Environment and Beijing Advanced Innovation Center for Big Data-Based Precision Medicine, Beihang University, Beijing 100191, China*

https://dx.doi.org/10.1021/acs.est.0c05095
Environ. Sci. Technol. 2021, 55, 1110−1121

Qihong Deng − *School of Energy Science and Engineering and Xiangya School of Public Health, Central South University, Changsha 410083, China;* orcid.org/0000-0001-9824-3534

Maigeng Zhou − *National Center for Chronic and Noncommunicable Disease Control and Prevention, Chinese Center for Disease Control and Prevention, Beijing 100050, China*

Complete contact information is available at: https://pubs.acs.org/10.1021/acs.est.0c05095

Author Contributions

#H.W. and P.Y. contributed equally to this work.

Notes

The authors declare no competing financial interest.

■ ACKNOWLEDGMENTS

This study was supported by the National Natural Science Foundation of China (Youth Program) [21707006] and the Fundamental Research Project of Beihang University [KG16036301]. The authors thank Dr. Jianping Guo for data sharing.

■ ABBREVIATIONS

all-cause	nonaccidental causes
CVD	cardiovascular diseases
CHD	coronary heart disease
RD	respiratory disease
COPD	chronic obstructive pulmonary disease
PM_1	particulate matter with an aerodynamic diameter less than or equal to 1 μm
$PM_{2.5}$	particulate matter with an aerodynamic diameter less than or equal to 2.5 μm
PM_{10}	particulate matter with an aerodynamic diameter less than or equal to 10 μm
$PM_{1-2.5}$	particulate matter with an aerodynamic diameter between 1 and 2.5 μm
$PM_{2.5-10}$	particulate matter with an aerodynamic diameter between 2.5 and 10 μm

■ REFERENCES

(1) Liu, C.; Chen, R.; Sera, F.; Vicedo-Cabrera, A. M.; Guo, Y.; Tong, S.; Coelho, M. S. Z. S.; Saldiva, P. H. N.; Lavigne, E.; Matus, P.; Ortega, N. V.; Garcia, S. O.; Pascal, M.; Stafoggia, M.; Scortichini, M.; Hashizume, M.; Honda, Y.; Hurtado-Díaz, M.; Cruz, J.; Nunes, B.; Teixeira, J. P.; Kim, H.; Tobias, A.; Íñiguez, C.; Forsberg, B.; Åström, C.; Ragettli, M. S.; Guo, Y. L.; Chen, B. Y.; Bell, M. L.; Wright, C. Y.; Scovronick, N.; Garland, R. M.; Milojevic, A.; Kyselý, J.; Urban, A.; Orru, H.; Indermitte, E.; Jaakkola, J. J. K.; Ryti, N. R. I.; Katsouyanni, K.; Analitis, A.; Zanobetti, A.; Schwartz, J.; Chen, J.; Wu, T.; Cohen, A.; Gasparrini, A.; Kan, H. Ambient Particulate Air Pollution and Daily Mortality in 652 Cities. *N. Engl. J. Med.* **2019**, *381*, 705−715.

(2) Samoli, E.; Stafoggia, M.; Rodopoulou, S.; Ostro, B.; Declercq, C.; Alessandrini, E.; Díaz, J.; Karanasiou, A.; Kelessis, A. G.; Tertre, A.; Le; Pandolfi, P.; Randi, G.; Scarinzi, C.; Zauli-Sajani, S.; Katsouyanni, K.; Forastiere, F.; Alessandrini, E.; Angelini, P.; Berti, G.; Bisanti, L.; Cadum, E.; Catrambone, M.; Chiusolo, M.; Davoli, M.; de' Donato, F.; Demaria, M.; Gandini, M.; Grosa, M.; Faustini, A.; Ferrari, S.; Forastiere, F.; Pandolfi, P.; Pelosini, R.; Perrino, C.; Pietrodangelo, A.; Pizzi, L.; Poluzzi, V.; Priod, G.; Randi, G.; Ranzi, A.; Rowinski, M.; Scarinzi, C.; Stafoggia, M.; Stivanello, E.; Zauli-Sajani, S.; Dimakopoulou, K.; Elefteriadis, K.; Katsouyanni, K.; G.Kelessis, A.; Maggos, T.; Michalopoulos, N.; Pateraki, S.; Petrakakis, M.; Rodopoulou, S.; Samoli, E.; Sypsa, V.; Agis, D.; Alguacil, J.; Artiñano, B.; Barrera-Gómez, J.; Basagaña, X.; de la Rosa, J.; Diaz, J.; Fernandez, R.; Jacquemin, B.; Karanasiou, A.; Linares, C.; Ostro, B.; Pérez, N.; Pey, J.; Querol, X.; Sanchez, A.; Sunyer, J.; Tobias, A.; Bidondo, M.; Declercq, C.; Le Tertre, A.; Lozano, P.; Medina, S.; Pascal, L.; Pascal, M. Associations between Fine and Coarse Particles and Mortality in Mediterranean Cities: Results from the MED-PARTICLES Project. *Environ. Health Perspect.* **2013**, *121*, 932−938.

(3) Zuo, J. X.; Ji, W.; Ben, Y. J.; Hassan, M. A.; Fan, W. H.; Bates, L.; Dong, Z. M. Using Big Data from Air Quality Monitors to Evaluate Indoor PM2.5 Exposure in Buildings: Case Study in Beijing. *Environ. Pollut.* **2018**, *240*, 839−847.

(4) Chen, R.; Yin, P.; Meng, X.; Wang, L.; Liu, C.; Niu, Y.; Liu, Y.; Liu, J.; Qi, J.; You, J.; Kan, H.; Zhou, M. Associations between Coarse Particulate Matter Air Pollution and Cause-Specific Mortality: A Nationwide Analysis in 272 Chinese Cities. *Environ. Health Perspect.* **2019**, *127*, 5−10.

(5) Yin, P.; Guo, J.; Wang, L.; Fan, W.; Lu, F.; Guo, M.; Moreno, S. B. R.; Wang, Y.; Wang, H.; Zhou, M.; Dong, Z. Higher Risk of Cardiovascular Disease Associated with Smaller Size-Fractioned Particulate Matter. *Environ. Sci. Technol. Lett.* **2020**, *7*, 95−101.

(6) Zanobetti, A.; Schwartz, J. The Effect of Fine and Coarse Particulate Air Pollution on Mortality: A National Analysis. *Environ. Health Perspect.* **2009**, *117*, 898−903.

(7) Zhang, Q.; Zheng, Y.; Tong, D.; Shao, M.; Wang, S.; Zhang, Y.; Xu, X.; Wang, J.; He, H.; Liu, W.; Ding, Y.; Lei, Y.; Li, J.; Wang, Z.; Zhang, X.; Wang, Y.; Cheng, J.; Liu, Y.; Shi, Q.; Yan, L.; Geng, G.; Hong, C.; Li, M.; Liu, F.; Zheng, B.; Cao, J.; Ding, A.; Gao, J.; Fu, Q.; Huo, J.; Liu, B.; Liu, Z.; Yang, F.; He, K.; Hao, J. Drivers of Improved PM2.5 Air Quality in China from 2013 to 2017. *Proc. Natl. Acad. Sci. U.S.A.* **2019**, *116*, 24463−24469.

(8) Chen, G.; Morawska, L.; Zhang, W.; Li, S.; Cao, W.; Ren, H.; Wang, B.; Wang, H.; Knibbs, L. D.; Williams, G.; Guo, J.; Guo, Y. Spatiotemporal Variation of PM1 Pollution in China. *Atmos. Environ.* **2018**, *178*, 198−205.

(9) Lin, Y.; Zou, J.; Yang, W.; Li, C. Q. A Review of Recent Advances in Research on PM2.5 in China. *Int. J. Environ. Res. Public Health* **2018**, *15*, No. 438.

(10) Kelly, F. J.; Fussell, J. C. Size, Source and Chemical Composition as Determinants of Toxicity Attributable to Ambient Particulate Matter. *Atmos. Environ.* **2012**, *60*, 504−526.

(11) Chen, R.; Zhou, B.; Kan, H.; Zhao, B. Associations of Particulate Air Pollution and Daily Mortality in 16 Chinese Cities: An Improved Effect Estimate after Accounting for the Indoor Exposure to Particles of Outdoor Origin. *Environ. Pollut.* **2013**, *182*, 278−282.

(12) Ni, Y.; Wu, S.; Ji, W.; Chen, Y.; Zhao, B.; Shi, S.; Tu, X.; Li, H.; Pan, L.; Deng, F.; Guo, X. The Exposure Metric Choices Have Significant Impact on the Association between Short-Term Exposure to Outdoor Particulate Matter and Changes in Lung Function: Findings from a Panel Study in Chronic Obstructive Pulmonary Disease Patients. *Sci. Total Environ.* **2016**, *542*, 264−270.

(13) Manigrasso, M.; Costabile, F.; Di, L.; Paolo, G.; Gualtieri, M.; Zanini, G.; Avino, P. Size Resolved Aerosol Respiratory Doses in a Mediterranean Urban Area: From PM10 to Ultra Fine Particles. *Environ. Int.* **2020**, *141*, No. 105714.

(14) Salma, I.; Füri, P.; Németh, Z.; Balásházy, I.; Hofmann, W.; Farkas, Á. Lung Burden and Deposition Distribution of Inhaled Atmospheric Urban Ultrafine Particles as the First Step in Their Health Risk Assessment. *Atmos. Environ.* **2015**, *104*, 39−49.

(15) Quintana-Belmares, R. O.; Krais, A. M.; Esfahani, B. K.; Rosas-Pérez, I.; Mucs, D.; López-Marure, R.; Bergman, Å.; Alfaro-Moreno, E. Phthalate Esters on Urban Airborne Particles: Levels in PM10 and PM2.5 from Mexico City and Theoretical Assessment of Lung Exposure. *Environ. Res.* **2018**, *161*, 439−445.

(16) Hoek, G.; Kos, G.; Harrison, R.; de Hartog, J.; Meliefste, K.; ten Brink, H.; Katsouyanni, K.; Karakatsani, A.; Lianou, M.; Kotronarou, A.; Kavouras, I.; Pekkanen, J.; Vallius, M.; Kulmala, M.; Puustinen, A.; Thomas, S.; Meddings, C.; Ayres, J.; van Wijnen, J.; Hameri, K.

Indoor-Outdoor Relationships of Particle Number and Mass in Four European Cities. *Atmos. Environ.* **2008**, *42*, 156−169.
(17) Deng, Q.; Deng, L.; Miao, Y.; Guo, X.; Li, Y. Particle Deposition in the Human Lung: Health Implications of Particulate Matter from Different Sources. *Environ. Res.* **2019**, *169*, 237−245.
(18) Sánchez-Soberón, F.; Mari, M.; Kumar, V.; Rovira, J.; Nadal, M.; Schuhmacher, M. An Approach to Assess the Particulate Matter Exposure for the Population Living around a Cement Plant: Modelling Indoor Air and Particle Deposition in the Respiratory Tract. *Environ. Res.* **2015**, *143*, 10−18.
(19) Manojkumar, N.; Srimuruganandam, B.; Shiva Nagendra, S. M. Application of Multiple-Path Particle Dosimetry Model for Quantifying Age Specified Deposition of Particulate Matter in Human Airway. *Ecotoxicol. Environ. Saf.* **2019**, *168*, 241−248.
(20) Chen, R.; Yin, P.; Meng, X.; Liu, C.; Wang, L.; Xu, X.; Ross, J. A.; Tse, L. A.; Zhao, Z.; Kan, H.; Zhou, M. Fine Particulate Air Pollution and Daily Mortality: A Nationwide Analysis in 272 Chinese Cities. *Am. J. Respir. Crit. Care Med.* **2017**, *196*, 73−81.
(21) Dong, Z.; Wang, H.; Yin, P.; Wang, L.; Chen, R.; Fan, W.; Xu, Y.; Zhou, M. Time-Weighted Average of Fine Particulate Matter Exposure and Cause-Specific Mortality in China: A Nationwide Analysis. *Lancet Planet. Health* **2020**, *4*, e343−e351.
(22) Wei, J.; Li, Z.; Guo, J.; Sun, L.; Huang, W.; Xue, W.; Fan, T.; Cribb, M. Satellite-Derived 1-Km-Resolution PM1 Concentrations from 2014 to 2018 across China. *Environ. Sci. Technol.* **2019**, No. 13265.
(23) Liu, S.; Wu, X.; Lopez, A. D.; Wang, L.; Cai, Y.; Page, A.; Yin, P.; Liu, Y.; Li, Y.; Liu, J.; You, J.; Zhou, M. An Integrated National Mortality Surveillance System for Death Registration and Mortality Surveillance, China. *Bull. World Health Organ.* **2016**, *94*, 46−57.
(24) *International Statistical Classification of Diseases and Related Health Problems*; WHO. https://icd.who.int/browse10/2016/en (accessed Jun 2, 2020).
(25) *MPPD: Multiple-Path Particle Dosimetry Mode*; Associates Applied Research. https://www.ara.com/mppd/ (accessed Oct 13, 2020).
(26) Ham, W. A.; Ruehl, C. R.; Kleeman, M. J. Seasonal Variation of Airborne Particle Deposition Efficiency in the Human Respiratory System. *Aerosol Sci. Technol.* **2011**, *45*, 795−804.
(27) Yin, W.; Hou, J.; Xu, T.; Cheng, J.; Wang, X.; Jiao, S.; Wang, L.; Huang, C.; Zhang, Y.; Yuan, J. Association of Individual-Level Concentrations and Human Respiratory Tract Deposited Doses of Fine Particulate Matter with Alternation in Blood Pressure. *Environ. Pollut.* **2017**, *230*, 621−631.
(28) Li, X.; Yan, C.; Patterson, R. F.; Zhu, Y.; Yao, X.; Zhu, Y.; Ma, S.; Qiu, X.; Zhu, T.; Zheng, M. Modeled Deposition of Fine Particles in Human Airway in Beijing, China. *Atmos. Environ.* **2016**, *124*, 387−395.
(29) Sui, Z.; Zhang, Y.; Peng, Y.; Norris, P.; Cao, Y.; Pan, W. P. Fine Particulate Matter Emission and Size Distribution Characteristics in an Ultra-Low Emission Power Plant. *Fuel* **2016**, *185*, 863−871.
(30) Fan, X.; Liu, W.; Wang, G.; Lin, J.; Fu, Q.; Gao, S.; Li, Y. Size Distributions of Concentrations and Chemical Components in Hangzhou Atmospheric Particles. *China Environ. Sci.* **2011**, *31*, 13−18.
(31) Zhang, K.; Chai, F.; Zheng, Z.; Yang, Q.; Zhong, X.; Fomba, K. W.; Zhou, G. Size Distribution and Source of Heavy Metals in Particulate Matter on the Lead and Zinc Smelting Affected Area. *J. Environ. Sci.* **2018**, *71*, 188−196.
(32) Dong, Z.; Jiang, N.; Duan, S.; Zhang, L.; Li, S.; Zhang, R. Size Distributions and Size-Segregated Chemical Profiles of Particulate Matter in a Traffic Tunnel of East-Central China. *Atmos. Pollut. Res.* **2019**, *10*, 1873−1883.
(33) Hu, M.; Peng, J.; Sun, K.; Yue, D.; Guo, S.; Wiedensohler, A.; Wu, Z. Estimation of Size-Resolved Ambient Particle Density Based on the Measurement of Aerosol Number, Mass, and Chemical Size Distributions in the Winter in Beijing. *Environ. Sci. Technol.* **2012**, *46*, 9941−9947.
(34) Roy, M.; Becquemin, M. H.; Bouchikhi, A. Ventilation Rates and Lung Volumes for Lung Modelling Purposes in Ethnic Groups. *Radiat. Prot. Dosim.* **1991**, *38*, 49−55.
(35) ICRP. *Human Respiratory Tract Model for Radiological Protection: A Report of a Task Group of the International Commission on Radiological Protection*; Annals of the ICRP, 1994; pp 1−8.
(36) Stocks, J.; Quanjer, P. H. Reference Values for Residual Volume, Functional Residual Capacity and Total Lung Capacity: ATS Workshop on Lung Volume Measurements Official Statement of the European Respiratory Society. *Eur. Respir. J.* **1995**, *8*, 492−506.
(37) *Manual of the MPPD Model*; Associates Applied Research, 2015.
(38) Stuart, B. O. Deposition and Clearance of Inhaled Particles. *Environ. Health Perspect.* **1984**, *55*, 369−390.
(39) Ivanov, K. P. Circulation in the Lungs and Microcirculation in the Alveoli. *Respir. Physiol. Neurobiol.* **2013**, *187*, 26−30.
(40) Hammer, T.; Gao, H.; Pan, Z.; Wang, J. Relationship between Aerosols Exposure and Lung Deposition Dose. *Aerosol Air Qual. Res.* **2020**, *20*, 1083−1093.
(41) Chen, R.; Yin, P.; Wang, L.; Liu, C.; Niu, Y.; Wang, W.; Jiang, Y.; Liu, Y.; Liu, J.; Qi, J.; You, J.; Kan, H.; Zhou, M. Association between Ambient Temperature and Mortality Risk and Burden: Time Series Study in 272 Main Chinese Cities. *BMJ* **2018**, *363*, No. k4306.
(42) Shah, A. S. V.; Langrish, J. P.; Nair, H.; McAllister, D. A.; Hunter, A. L.; Donaldson, K.; Newby, D. E.; Mills, N. L. Global Association of Air Pollution and Heart Failure: A Systematic Review and Meta-Analysis. *Lancet* **2013**, *382*, 1039−1048.
(43) Whitehead, A. *Meta-Analysis Of Controlled Clinical Trials; Statistics in Practice*; John Wiley & Sons, Ltd: Chichester, U.K., 2002.
(44) Burnet t, R.; Chen, H.; Szyszkowicz, M.; Fann, N.; Hubbell, B.; Pope, C. A.; Apte, J. S.; Brauer, M.; Cohen, A.; Weichenthal, S.; Coggins, J.; Di, Q.; Brunekreef, B.; Frostad, J.; Lim, S. S.; Kan, H.; Walker, K. D.; Thurston, G. D.; Hayes, R. B.; Lim, C. C.; Turner, M. C.; Jerrett, M.; Krewski, D.; Gapstur, S. M.; Diver, W. R.; Ostro, B.; Goldberg, D.; Crouse, D. L.; Martin, R. V.; Peters, P.; Pinault, L.; Tjepkema, M.; Van Donkelaar, A.; Villeneuve, P. J.; Miller, A. B.; Yin, P.; Zhou, M.; Wang, L.; Janssen, N. A. H.; Marra, M.; Atkinson, R. W.; Tsang, H.; Thach, T. Q.; Cannon, J. B.; Allen, R. T.; Hart, J. E.; Laden, F.; Cesaroni, G.; Forastiere, F.; Weinmayr, G.; Jaensch, A.; Nagel, G.; Concin, H.; Spadaro, J. V. Global Estimates of Mortality Associated with Longterm Exposure to Outdoor Fine Particulate Matter. *Proc. Natl. Acad. Sci. U.S.A.* **2018**, *115*, 9592−9597.
(45) Vandyck, T.; Keramidas, K.; Kitous, A.; Spadaro, J. V.; Van Dingenen, R.; Holland, M.; Saveyn, B. Air Quality Co-Benefits for Human Health and Agriculture Counterbalance Costs to Meet Paris Agreement Pledges. *Nat. Commun.* **2018**, *9*, No. 1345.
(46) Hu, K.; Guo, Y.; Hu, D.; Du, R.; Yang, X.; Zhong, J.; Fei, F.; Chen, F.; Chen, G.; Zhao, Q.; Yang, J.; Zhang, Y.; Chen, Q.; Ye, T.; Li, S.; Qi, J. Mortality Burden Attributable to PM1 in Zhejiang Province, China. *Environ. Int.* **2018**, *121*, 515−522.
(47) Lu, F.; Xu, D.; Cheng, Y.; Dong, S.; Guo, C.; Jiang, X.; Zheng, X. Systematic Review and Meta-Analysis of the Adverse Health Effects of Ambient PM2.5 and PM10 Pollution in the Chinese Population. *Environ. Res.* **2015**, *136*, 196−204.
(48) Chen, R.; Peng, R. D.; Meng, X.; Zhou, Z.; Chen, B.; Kan, H. Seasonal Variation in the Acute Effect of Particulate Air Pollution on Mortality in the China Air Pollution and Health Effects Study (CAPES). *Sci. Total Environ.* **2013**, *450*−*451*, 259−265.
(49) Peng, R. D.; Dominici, F.; Pastor-Barriuso, R.; Zeger, S. L.; Samet, J. M. Seasonal Analyses of Air Pollution and Mortality in 100 US Cities. *Am. J. Epidemiol.* **2005**, *161*, 585−594.
(50) Ebenstein, A.; Fan, M.; Greenstone, M.; He, G.; Zhou, M. New Evidence on the Impact of Sustained Exposure to Air Pollution on Life Expectancy from China's Huai River Policy. *Proc. Natl. Acad. Sci. U.S.A.* **2017**, *114*, 10384−10389.
(51) Chen, Y.; Ebenstein, A.; Greenstone, M.; Li, H. Evidence on the Impact of Sustained Exposure to Air Pollution on Life Expectancy from China's Huai River Policy. *Proc. Natl. Acad. Sci. U.S.A.* **2013**, *110*, 12936−12941.

https://dx.doi.org/10.1021/acs.est.0c05095
Environ. Sci. Technol. 2021, 55, 1110−1121

(52) Heyder, J.; Gebhart, J.; Rudolf, G.; Schiller, C. F.; Stahlhofen, W. Deposition of Particles in the Human Respiratory Tract in the Size Range 0.005−15 Mm. *J. Aerosol Sci.* **1986**, *17*, 811−825.
(53) Shen, F.; Zheng, Y.; Niu, M.; Zhou, F.; Wu, Y.; Wang, J.; Zhu, T.; Wu, Y.; Wu, Z.; Hu, M.; Zhu, T. Characteristics of Biological Particulate Matters at Urban and Rural Sites in the North China Plain. *Environ. Pollut.* **2019**, *253*, 569−577.
(54) Wang, H.; Lu, F.; Guo, M.; Fan, W.; Ji, W.; Dong, Z. Associations between PM1 Exposure and Daily Emergency Department Visits in 19 Hospitals, Beijing. *Sci. Total Environ.* **2020**, *755*, No. 142507.
(55) Sinharay, R.; Gong, J.; Barratt, B.; Ohman-Strickland, P.; Ernst, S.; Kelly, F. J.; Zhang, J. Jim.; Collins, P.; Cullinan, P.; Chung, K. F. Respiratory and Cardiovascular Responses to Walking down a Traffic-Polluted Road Compared with Walking in a Traffic-Free Area in Participants Aged 60 Years and Older with Chronic Lung or Heart Disease and Age-Matched Healthy Controls: A Randomised, Crosso. *Lancet* **2018**, *391*, 339−349.
(56) Zhou, M.; Wang, H.; Zeng, X.; Yin, P.; Zhu, J.; Chen, W.; Li, X.; Wang, L.; Wang, L.; Liu, Y.; Liu, J.; Zhang, M.; Qi, J.; Yu, S.; Afshin, A.; Gakidou, E.; Glenn, S.; Krish, V. S.; Miller-Petrie, M. K.; Mountjoy-Venning, W. C.; Mullany, E. C.; Redford, S. B.; Liu, H.; Naghavi, M.; Hay, S. I.; Wang, L.; Murray, C. J. L.; Liang, X. Mortality, Morbidity, and Risk Factors in China and Its Provinces, 1990−2017: A Systematic Analysis for the Global Burden of Disease Study 2017. *Lancet* **2019**, *394*, 1145−1158.
(57) Anenberg, S. C.; Horowitz, L. W.; Tong, D. Q.; West, J. J. An Estimate of the Global Burden of Anthropogenic Ozone and Fine Particulate Matter on Premature Human Mortality Using Atmospheric Modeling. *Environ. Health Perspect.* **2010**, *118*, 1189−1195.
(58) Yan, M.; Wilson, A.; Bell, M. L.; Peng, R. D.; Sun, Q.; Pu, W.; Yin, X.; Li, T.; Anderson, G. B. The Shape of the Concentration—Response Association between Fine Particulate Health Impact Assessment. *Environ. Health Perspect.* **2019**, *127*, No. 067007.
(59) Cox, L. A. Effects of Exposure Estimation Errors on Estimated Exposure-Response Relations for PM2.5. *Environ. Res.* **2018**, *164*, 636−646.
(60) Wang, R.; Tao, S.; Wang, W.; Liu, J.; Shen, H.; Shen, G.; Wang, B.; Liu, X.; Li, W.; Huang, Y.; Zhang, Y.; Lu, Y.; Chen, H.; Chen, Y.; Wang, C.; Zhu, D.; Wang, X.; Li, B.; Liu, W.; Ma, J. Black Carbon Emissions in China from 1949 to 2050. *Environ. Sci. Technol.* **2012**, *46*, 7595−7603.
(61) WHO. Health Effects of Black Carbon. https://www.euro.who.int/__data/assets/pdf_file/0004/162535/e96541.pdf (accessed Oct 13, 2020).
(62) Janssen, N. A. H.; Hoek, G.; Simic-Lawson, M.; Fischer, P.; van Bree, L.; Brink, H.; Ten; Keuken, M.; Atkinson, R. W.; Ross Anderson, H.; Brunekreef, B.; Cassee, F. R. Black Carbon as an Additional Indicator of the Adverse Health Effects of Airborne Particles Compared with PM10 and PM2.5. *Environ. Health Perspect.* **2011**, *119*, 1691−1699.
(63) Chen, G.; Li, S.; Zhang, Y.; Zhang, W.; Li, D.; Wei, X.; He, Y.; Bell, M. L.; Williams, G.; Marks, G. B.; Jalaludin, B.; Abramson, M. J.; Guo, Y. Effects of Ambient PM1 Air Pollution on Daily Emergency Hospital Visits in China: An Epidemiological Study. *Lancet Planet. Health* **2017**, *1*, e221−e229.
(64) Wang, C.; Chen, R.; Zhao, Z.; Cai, J.; Lu, J.; Ha, S.; Xu, X.; Chen, X.; Kan, H. Particulate Air Pollution and Circulating Biomarkers among Type 2 Diabetic Mellitus Patients: The Roles of Particle Size and Time Windows of Exposure. *Environ. Res.* **2015**, *140*, 112−118.
(65) Ben, Y. J.; Ma, J.; Wang, H.; Hassan, M. A.; Yevheniia, R.; Fan, W. H.; Li, Y.; Dong, Z. M. A Spatio-Temporally Weighted Hybrid Model to Improve Estimates of Personal PM2.5 Exposure: Incorporating Big Data from Multiple Data Sources. *Environ. Pollut.* **2019**, *253*, 403−411.

https://dx.doi.org/10.1021/acs.est.0c05095
Environ. Sci. Technol. 2021, 55, 1110−1121